50th International Annual Conference of the Fraunhofer ICT
June 25 – June 28, 2019, Karlsruhe, Germany

SAND2019-5488C

Meso-scale and continuum simulations for Arrhenius reactive burn model calibration of initiation in hexanitrostilbene (HNS)

Joseph D. Olles[1], Graham D. Kosiba[2], Cole Yarrington[1], and Ryan R. Wixom[1]

[1]Sandia National Laboratories, Albuquerque, NM, U.S.A.
[2]Lawrence Livermore National Laboratory, Livermore, CA, U.S.A.

Abstract

Modeling the initiation of explosives requires that many physical phenomena be captured and represented as accurately as possible. Chemical processes and energy release during run-to-detonation are especially challenging to capture. These processes can be modeled with detailed or global kinetic mechanisms or more analytical models. Excluding a detailed kinetic mechanism, each model requires empirical calibration. Experimental data providing particle velocity as a function of time or distance within the explosive is particularly useful for calibrating chemical models. This data is often collected by cutbacks of pressed powder-beds or embedded gauge experiments, however hexanitrostilbene (HNS) exhibits growth to detonation in spatial distances which are too short to be captured by those traditional experiments. Recently, an advanced manufacturing technique of physical vapor-deposition allowed for the creation of HNS films of precisely controlled thicknesses. These new cutback experiments were initiated with electrically driven flyers and particle velocity data for the flyer flight, impact, and shock duration was obtained via PDV. Here, we utilize that experimental data to calibrate a single-step Arrhenius reaction rate for HNS decomposition.

Several simulations were designed and used for calibration of the Arrhenius equation parameters with Sandia's shock physics hydrocode, CTH. The HNS was modeled in both continuum and with representative microstructure. In continuum, the HNS is a homogenous material of prescribed density. To include microstructure, a HNS sample was cross-sectioned and faced with an ion-beam and imaged with a Scanning Electron Microscope (SEM). A binary image from this electron micrograph was directly imported as the HNS in CTH. The experimental materials and setup geometry were replicated in one, two, and three dimensional simulations. The effects of higher simulation dimensionality on properties, such as particle velocity, in the HNS within an area equal to the PDV probe was investigated. Evaluation of the Arrhenius equation parameters was performed by varying the pre-exponential factor and minimizing a designed objective function. The objective function consists of the sum of squares error between the experimental and simulation particle velocity trace at equivalent time increments. A fifteen nanosecond time band beginning at impact, sampled every 0.1 nanoseconds, was used in quantifying the error for optimization. The resulting simulations with calibrated Arrhenius reactive model show good agreement with experimental data.

1 Introduction

The chemical reactions that release energy during the run-to-detonation are challenging to measure due to the short length scales (10s-100s of microns) and fast time scales (10s-1000s of picoseconds) at which they occur. These processes can be modeled with detailed or global kinetic mechanisms or more analytical models, such as reactive burn or growth models.[1,2] Most of these reaction models require an empirical calibration. Experimental data of particle velocity as a function of time or distance within the explosive is one means for calibrating reaction models. This data is often collected by cutback or embedded gauge experiments, however HNS exhibits run-to-detonation in spatial distances which are too short ($\sim$100 μm) to be captured by those experiments.[3] Recently, thin vapor-deposited hexanitrostilbene (HNS) films of increasing thicknesses were initiated with electrically driven flyers[4]. Particle velocity data for the flyer flight, impact, and shock duration was obtained via PDV.[5] This work seeks to utilize that experimental data to calibrate a single-step Arrhenius reaction rate for HNS shock to detonation transition.

In order to have confidence in the simulations to interpolated regions, where experimental data was not used for calibration, the reactions in localized regions needs to be accounted for. The material's size and shape of the internal porosity is a key property that will influence the kinetics. The microstructure of the prepared HNS has been shown to have a direct relation to the behavior after impact, including, run-to-detonation distances.[6,7] The mechanism of run-to-detonation has also been shown to differ in homogeneous versus heterogeneous explosive initiation simulations.[8] There are several proposed explanations for shock to detonation transition, with the most commonly put forward explanation being hot-spot theory. These small, localized high temperature regions are observed in the simulations and it follows that the overarching phenomenon is roughly captured when utilizing the temperature dependent Arrhenius equation. Additionally, the geometry and dimensionality of the simulations impact the applicability of the results and has been accounted for and studied during calibration.

2 Experimental Methodology

The short distance for run-to-detonation in HNS excludes the use of conventional embedded gauge or cutback tests for measuring initiation properties necessary for development of a reactive burn model. However, a physical vapor deposition process for HNS has been developed which allows for sub-millimeter explosive samples.[4] There is a degree of control over the deposition process which results in desired film thickness and microstructure characteristics. This means that HNS samples can be made which have thicknesses near the expected run-distance, ($\sim$100 μm). Experiments which initiate the thin films with an electrically driven flyer and measure the flight of the flyer with frequency shifted photon Doppler velocimetry (PDV) were able to determine the run-to-detonation in HNS.[5] These data, which may be the first direct measurements of run-to-detonation at these scales, were used to calibrate an Arrhenius burn model for the initiation of HNS.

A 2μm aluminum film was first deposited on the acrylic substrate (PMMA). The aluminum provides a reflective surface for the PDV measurement. HNS was then deposited onto the aluminum film using a high-vacuum deposition system. The thickness of the resulting film was controlled and samples were produced with thicknesses of 30-150 μm in 30 μm increments. These films were initiated by 50 μm thick Parylene-C flyers driven by exploding 2.54 x 2.54 mm metal foil bridges. A high voltage discharge unit vaporizes the metal foil bridge, accelerating the plastic flyer to several km/s which impacts a free surface of the HNS film. In these experiments, the particle velocity history at the aluminum film and acrylic substrate interface was recorded via frequency shifted PDV with a collimated gradient-index probe with spot size of 0.5 mm.[5] A schematic of the experimental setup from Olles *et al.* is shown in Figure 1.[5]

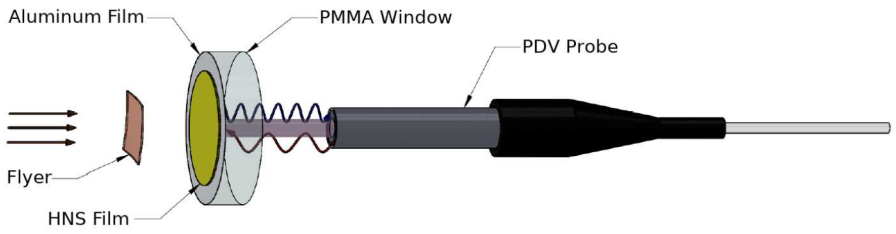

Figure 1: Schematic of experiment.[5]

3 Modeling Methodology

Several simulations were designed and used for calibration of the Arrhenius equation parameters with Sandia's hydrocode CTH.[9] The experimental setup described above was replicated in one and two-dimensional simulations. Additionally, in experiments, the flyer accelerates through a gap filled with air until impact with the explosive. This flight of the flyer through air was investigated in simulation and an approximation of the acceleration profile was implemented. Thus, simulations may consist of three or four materials: PMMA, HNS, Parylene-C, and Air (if included). The Parylene-C flyer equation of state (EOS) was implemented in CTH with a Mie-Gruneisen analytical model.[10] The PMMA window, air, and reacted HNS equations of state were implemented as sesame tables built from thermochemical equilibrium calculations.[11] The unreacted HNS equation of state was developed previously with density

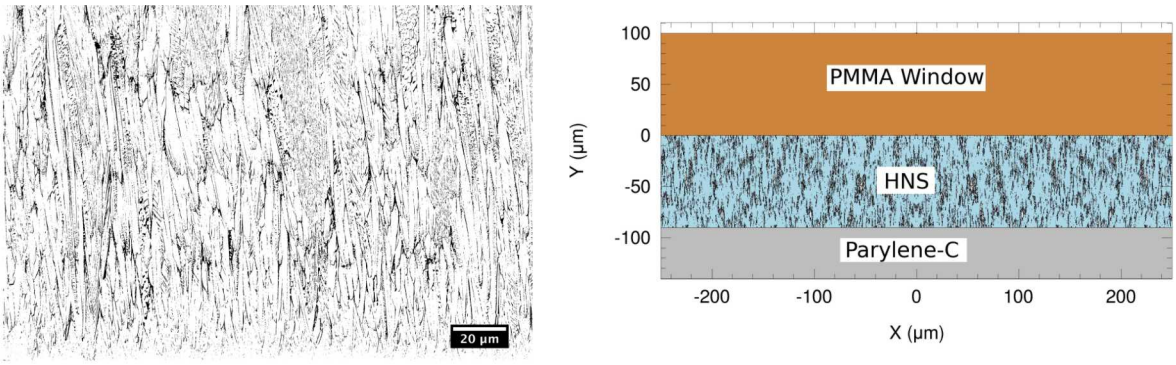

Figure 2: Binary SEM image of ion-beam faced HNS film (left). Example 2D simulation geometry with inserted microstructure (right).

functional theory molecular dynamics (DFT-MD).[8] The HNS was modeled in both continuum and with representative microstructure. In continuum, the HNS is a homogeneous material of prescribed density. To include microstructure, an HNS sample was cross-sectioned and polished with an ion-beam and imaged with a Scanning Electron Microscope (SEM). A binary image from this electron micrograph was directly imported as the HNS in CTH. An example of a binary image of the HNS micrograph and the two-dimensional simulation setup with HNS microstructure is shown in Figure 2.

In the experiment, the particle velocity measurement is determined from an area which is limited to the probe spot size. The effects of higher simulation dimensionality on properties, such as particle velocity, in the HNS within an area equal to the PDV probe was investigated. It was found that in the two and three-dimensional continuum cases the response within the HNS appears one-dimensional, in an area equivalent to the PDV probe. Then, the overall simulation domain can be reduced, improving computation time. When microstructure is included, the behavior after impact requires resolution of the higher dimensional effects. Properly capturing the effects of the microstructure includes understanding the effect of size and distribution of included pores, *i.e.* the response following a single large pore is different than a grouping of small pores. For use in a calibration simulation, it is critical that the net behavior arising from microstructure is not a function of the simulation domain.[8] Additionally, this lends itself to interesting macro- vs meso-scale studies with a calibrated reactive model.

An Arrhenius equation for a temperature dependent reaction rate, shown in Equation 1, consists of two empirical parameters, the pre-exponential factor or frequency factor (FF) and the activation temperature (AT).

$$k = FF \exp\left(\frac{-AT}{T}\right) \tag{1}$$

The activation temperature was fixed at a value which was previously determined in molecular dynamics (MD) simulations.[12] Calibration of the Arrhenius equation pre-exponential factor was performed by varying the value and minimizing a designed objective function. The objective function consists of the sum of squares error between the experimental and simulation particle velocity trace at equivalent time increments. A fifteen nanosecond time band beginning at impact, sampled every 0.1 nanoseconds, was used in quantifying the error for optimization.

4 Results

4.1 Effects of Dimensionality

There is significant computational cost increase moving between one, two, or three-dimensional simulations. A balance between minimizing computational cost and capturing relevant physics in simulations must be made. In flyer impacts, higher dimensional effects may arise at the edges of the flyer and at domain boundaries with boundary conditions as they are assigned. However, the experimental data described above is captured by a PDV probe with a spot size of 0.5mm. The spot size, centered on the plastic flyer, is significantly smaller than the flyer itself. The shock front traveling through the material in continuum simulations is one-dimensional as observed in an area equivalent to the PDV probe. Figure 3 illustrates this, depicting a particle velocity trace at the HNS-PMMA interface in the center of the flyer for a one and two-dimensional simulation. For explosive initiation by flyer impact, the flyer

area, thickness, and impact velocity account for the critical ignition condition or threshold and there is likely appreciable difference between one and two-dimensional simulations near this threshold.[6,13] In addition to the PDV spot-size versus flyer dimension resulting in no edge effects as discussed above, the flyer thickness (50 μm) and impact velocity (3.1 km/s) used in the experiment and simulations here are well above the critical ignition condition.[13,14] Then the calibration of Arrhenius parameters without microstructure can be performed as one-dimensional simulations, which are significantly cheaper than equivalent two-dimensional simulations (∼450 s vs ∼2000 s at each calibration point).

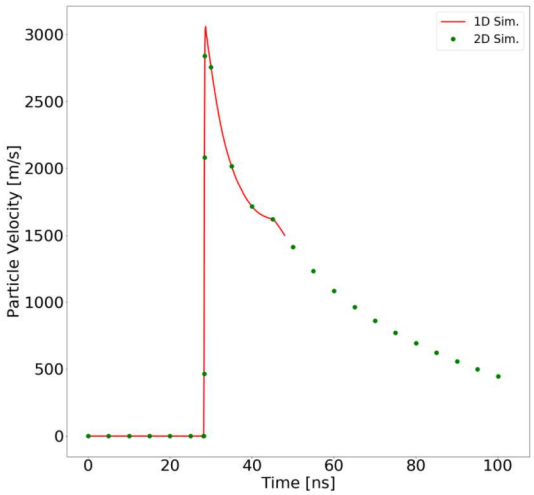

Figure 3: Particle velocity trace in one and two-dimensional simulations are indistinguishable, demonstrating one-dimensionality in area of interest equivalent to PDV probe spot size for calibration simulations at impact velocity above threshold.

4.2 Air Gap Effects

In the experiment, there is a gap between the exploding bridge which accelerates the flyer and the surface of the explosive which is impacted. Simulations were done to study the effect of this gap which is filled with air. A schematic of the one-dimensional simulation is presented in Figure 4 (left). The flyer traveling through the air generates a bow shock ahead of the flyer, shown in Figure 4 (right).

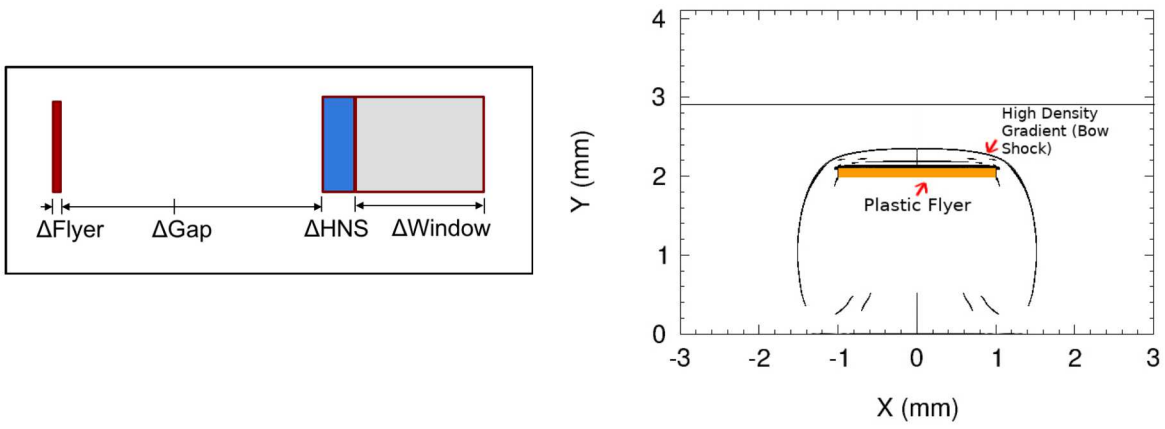

Figure 4: CTH input geometry sketch. (left). Density gradient field. Gradient values clipped to only display large gradients (shocks) (right).

This pressure front impacts the HNS film ahead of the plastic flyer and pre-shocks the material, to ∼10 MPa. Although this pressure is low relative to the peak pressure from the flyer impact, it was found to have a significant effect on the impact response of the HNS. Figure 5 presents the calibration minima

and particle velocity trace overlay for simulation and experiment in the case where there is no air in the gap and thus no pre-compressed HNS. Figure 6 presents the calibration minima and particle velocity trace overlay for the case where there is air in the gap and thus the flyer impacts pre-compressed HNS.

The presence of air and thus the flyer's impact into pre-compressed HNS drastically changes the impact response of the explosive. The particle velocity traces of the simulation with air have less error when compared to the experiment, suggesting this is an important physical phenomenon which should be included in simulations, despite increased computational costs. A compression wave desensitizes an explosive and this trend is observed in the resulting calibrated Arrhenius parameters, for the same conditions, a higher reaction rate optimization solution is found when the HNS has been desensitized. In other words, for the same film thickness, the desensitized HNS requires a faster reaction rate to reach detonation than the uncompressed explosive.

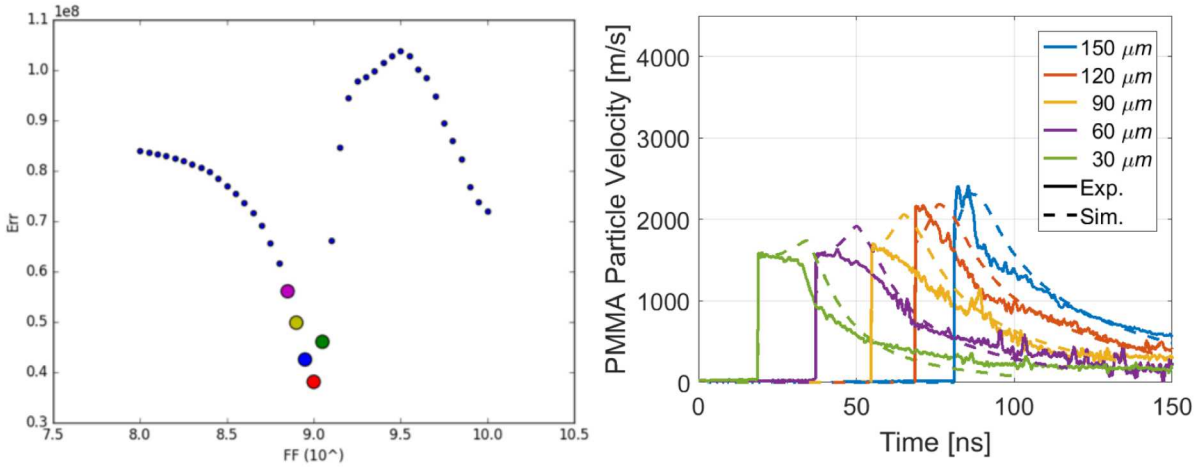

Figure 5: One-dimensional flyer impact simulation without presence of air. FF and AT parameter calibration space, with minima highlighted (left). Experiment and simulation particle velocity traces overlay with calibrated Arrhenius parameters (right).

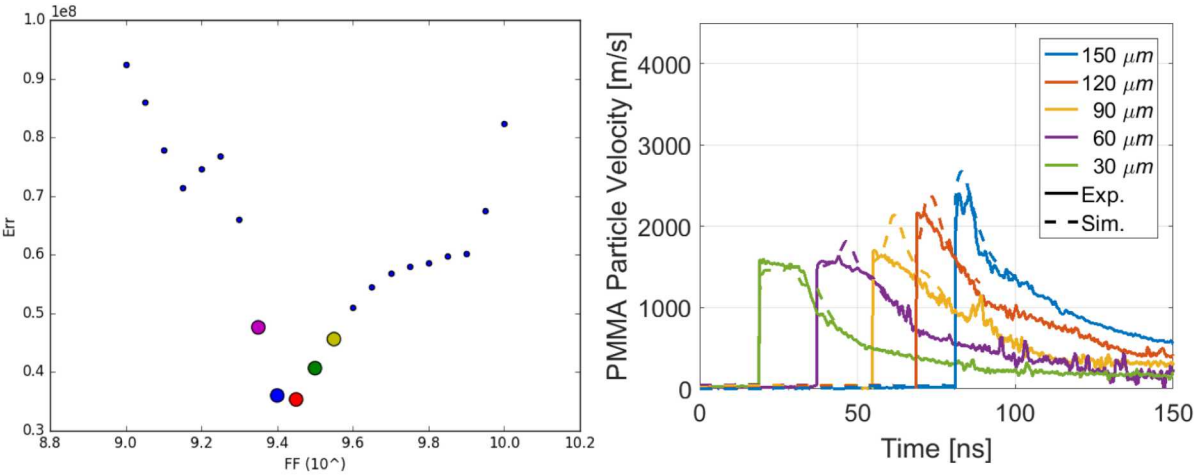

Figure 6: One-dimensional flyer impact simulation with presence of air. FF and AT parameter calibration space, with minima highlighted (left). Experiment and simulation particle velocity traces overlay with calibrated Arrhenius parameters (right).

4.3 Microstructure Effects

The microstructure of the prepared HNS has been shown to have a direct influence on the behavior after impact, including, run-to-detonation distances. To evaluate HNS in predictive hydrocode simulations it is important to include some representative microstructure, but also consider how constitutive models

may now fall outside their original empirical calibration with the addition of the microstructure. Here, the same Arrhenius parameters are calibrated from a series of simulations which include a representative microstructure. A thin vapor deposited HNS film was ion polished and imaged with an SEM. The resulting image, after post-processing, was imported into CTH as the HNS directly. In some cases, the bounds of the micrograph are smaller than the HNS which is being modeled. For these cases, the image is tiled and stitched together to reach the desired dimensions. The pores in the films have very small aspect ratio, appearing as vertical strips. In the minor direction the pore is quite small, on the order of 0.5 μm, necessitating very fine mesh resolution. A view of the two-dimensional pressure field after flyer impact is shown in Figure 7. Unlike the continuum case, the shock front is not expected to be perfectly planar,

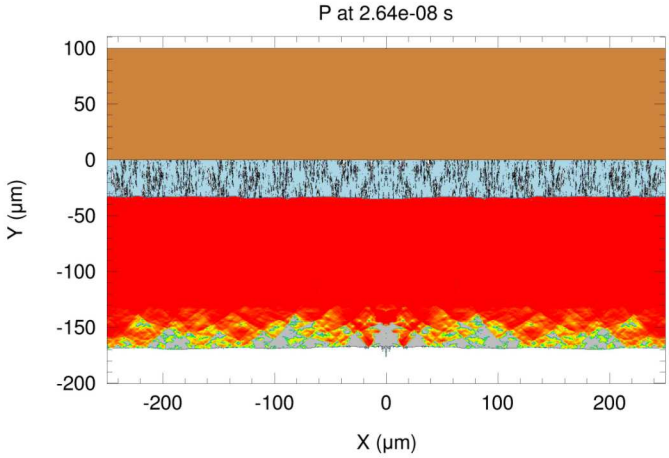

Figure 7: Pressure field after flyer impact.

making it critical to consider the particle velocity from multiple cells. All cells which fall in the 0.5 mm PDV probe spot size at the HNS-PMMA interface are averaged to find a final value. Figure 8 shows an example variation in particle velocity at each cell. The average velocity value across the spot size is used for the calibration and experimental data comparison, shown in Figure 9. The introduction of the microstructure in the HNS resulted in new calibrated Arrhenius parameters that had better agreement with the experimental data than the homogeneous HNS. The localized heating at crushed pores results in higher reaction rates and is a more accurate representation of the experiment.

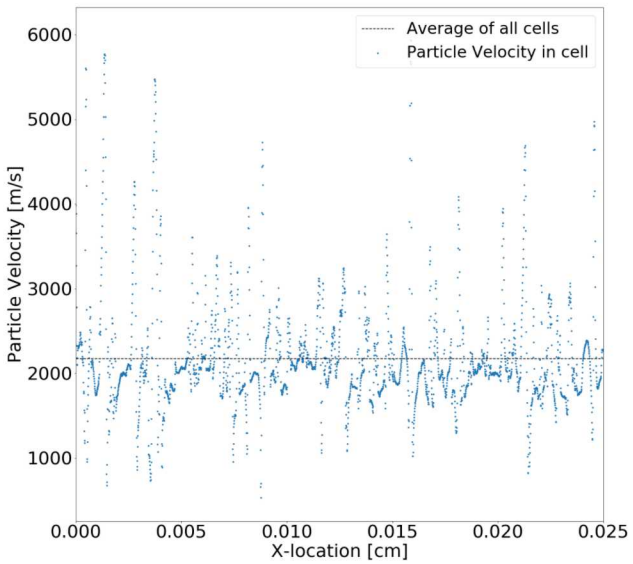

Figure 8: Particle velocity at every cell at HNS-PMMA interface in PDV probe spot-size.

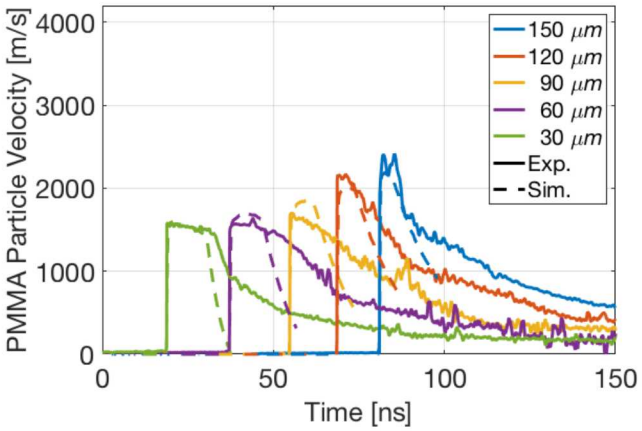

Figure 9: Experiment and full microstructural simulation particle velocity traces overlay with calibrated Arrhenius parameters (AT=0.42, FF=$10^{9.3}$).

5 Conclusions

The resulting simulations with calibrated Arrhenius reactive model show good agreement with experimental data. In the continuum case and at conditions above initiation threshold, the response within the HNS appears one-dimensional in an area equivalent to the PDV probe. However, when microstructure is included, the behavior after impact requires resolution of the higher dimensional effects. A group of cells which represent the PDV probe were averaged for use in the optimization. The inclusion of microstructure greatly improved the comparison of the simulated run-to-detonation results. Simulations were done to study the effect of the flyer accelerating through an air gap prior to impact with the explosive. The flyer traveling through the air generates a bow shock and this pressure front impacts the HNS film ahead of the plastic flyer, pre-compressing the material. The pre-compression desensitizes the explosive and changes the Arrhenius parameters found to optimize the run-to-detonation response of the model. The variations in calibrated Arrhenius parameters depending on simulation design highlights the care which must be taken when incorporating empirical models in predictive calculations. The resulting burn model shows good agreement with run to detonation experimental results which were previously unavailable. Further investigation of HNS initiation, including threshold, with the improved models is on-going.

6 Acknowledgments

The authors would like to thank J. Patrick Ball, Michael Marquez, and Robert Knepper for their work in sample preparation and experimental data collection.
This work was performed, in part, at the Center for Integrated Nanotechnologies, an Office of Science User Facility operated for the U.S. Department of Energy (DOE) Office of Science. Sandia National Laboratories is a multimission laboratory managed and operated by National Technology & Engineering Solutions of Sandia, LLC, a wholly owned subsidiary of Honeywell International, Inc., for the U.S. DOE's National Nuclear Security Administration under contract DE-NA-0003525. The views expressed in the article do not necessarily represent the views of the U.S. DOE or the United States Government.
Lawrence Livermore National Laboratory is operated by Lawrence Livermore National Security, LLC, for the U.S. Department of Energy, National Nuclear Security Administration under Contract DE-AC52-07NA27344. LLNL-PROC-754222

References

[1] ES Hertel and GI Kerley. Cth eos package. *SAND98-0945, Sandia National Laboratories, Albuquerque, NM*, 1998.

[2] Edward L Lee and Craig M Tarver. Phenomenological model of shock initiation in heterogeneous explosives. *The Physics of Fluids*, 23(12):2362–2372, 1980.

[3] Ryan R Wixom, Cole D Yarrington, Robert Knepper, Alexander S Tappan, Joseph D Olles, and David L Damm. Characterizing the growth to detonation in hns with small-scale pdv "cutback" experiments. In *AIP Conference Proceedings*, volume 1793, page 160001. AIP Publishing, 2017.

[4] Robert Knepper, Ryan R Wixom, Michael P Marquez, and Alexander S Tappan. Near-failure detonation behavior of vapor-deposited hexanitrostilbene (hns) films. In *AIP Conference Proceedings*, volume 1793, page 030014. AIP Publishing, 2017.

[5] Joseph D Olles, Ryan R Wixom, Robert Knepper, Alexander S Tappan, and Cole Yarrington. Growth to detonation in hexanitrostilbene (hns). Technical report, Sandia National Lab.(SNL-NM), Albuquerque, NM (United States), 2016.

[6] Alfred C Schwarz. Shock initiation sensitivity of hexanitrostilbene (hns). Technical report, Sandia National Labs., Albuquerque, NM (USA), 1981.

[7] Alfred C Schwarz. Study of factors which influence the shock-initiation sensitivity of hexanitrostilbene (hns). Technical report, Sandia National Labs., Albuquerque, NM (USA), 1981.

[8] Cole D Yarrington, Ryan R Wixom, and David L Damm. Shock interactions with heterogeneous energetic materials. *Journal of Applied Physics*, 123(10):105901, 2018.

[9] J Michael McGlaun, SL Thompson, and MG Elrick. Cth: a three-dimensional shock wave physics code. *International Journal of Impact Engineering*, 10(1-4):351–360, 1990.

[10] Chadd M May and Craig M Tarver. Modeling short shock pulse duration initiation of lx-16 and lx-10 charges. In *AIP Conference Proceedings*, volume 1195, pages 275–278. AIP, 2009.

[11] M Cowperthwaite and WH Zwisler. Tiger computer program documentation. *Z106, January*, 1973.

[12] Personal communication from Ryan Wixom and Ray Shan, Sandia National Laboratories, 2017.

[13] EJ Welle, CD Molek, RR Wixom, and P Samuels. Microstructural effects on the ignition behavior of hmx. In *Journal of Physics: Conference Series*, volume 500, page 052049. IOP Publishing, 2014.

[14] Mike D Bowden and Matthew P Maisey. Determination of critical energy criteria for hexanitrostilbene using laser-driven flyer plates. In *Optical Technologies for Arming, Safing, Fuzing, and Firing IV*, volume 7070, page 707004. International Society for Optics and Photonics, 2008.